2 A. R. Eberle, M. W. Lerner, C. G. Goldbeck and C. J. Rodden, *NBL-252*, (1970).
3 M. Davies and M. Townsend, *TRG Report 2453 (D)*, (1974).
4 J. R. Flanary, J. H. Goode, M. J. Bradley, J. W. Ullmann, L. M. Ferris and G. C. Wall, *ORNL-3660*, (1964).
5 R. E. Manzoni, *Diplomarbeit*, Saarbrücken 1981.
6 G. R. Choppin, H. Bokelund and S. Valkiers, *Radiochim. Acta*, in press.
7 G. R. Choppin, H. Bokelund, M. S. Caceci and S. Valkiers, *Radiochim. Acta*, submitted.
8 H. Bokelund, M. Caceci and W. Müller, *Radiochim. Acta*, in press.

## E10

## The Use of RE-O-S Phase Stability Diagrams in Gaseous Desulfurisation and Iron and Steel Production

D. A. R. KAY*, S. V. SUBRAMANIAN, V. KUMAR and V. MENG

*Department of Metallurgy and Materials Science, McMaster University, Hamilton, Ont., Canada*

R. K. DWIVEDI

*Ontario Research Foundation, Mississauga, Ont., Canada*

The thermodynamic properties of rare earth (RE) compounds containing oxygen and/or sulfur are of industrial significance in the high temperature desulfurisation of gaseous fuels by rare earth oxides [1], the control of graphite morphology in cast irons [2] and sulfide inclusion control in steels [1]. The initial form of the phase stability diagrams was based on the thermochemical data of Gschneidner *et al.* [3] using cerium as a 'representative' rare earth [4]. More recently [5], the high temperature standard free energies of formation of some RE–O–S compounds have been determined using oxygen concentration cells with calcia stabilised zirconia (CSZ) as the solid electrolyte, and the phase stability diagrams extended to higher oxygen potentials.

*The La–O–S and Ce–O–S Diagrams.* Updated versions of the La–O–S and Ce–O–S phase stability diagrams at 1100 K [5] are given in Fig. 1 and 2, respectively.

For the La–O–S diagram, oxygen concentration cells of the type:

$Pt/La_2O_3(s), La_2O_2S(s), La_2O_2SO_4(s)/CSZ/Air/Pt$ and $Pt/La_2O_2S(s), La_2O_2SO_4(s), Ag(s), Ag_2S(s)/CSZ/Air/Pt$ were used [5] to generate thermodynamic data on the equilibrium:

$$La_2O_2S(s) + 2O_2(g) = La_2O_2SO_4(s) \quad (1)$$

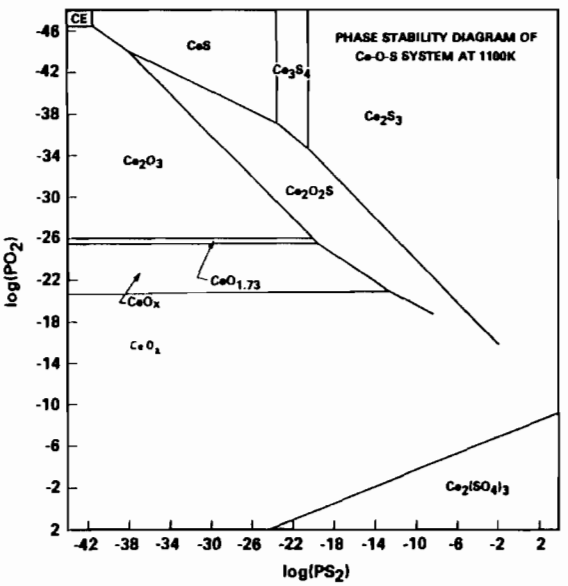


Fig. 2. The Ce–O–S phase stability diagram at 1100 K [5].

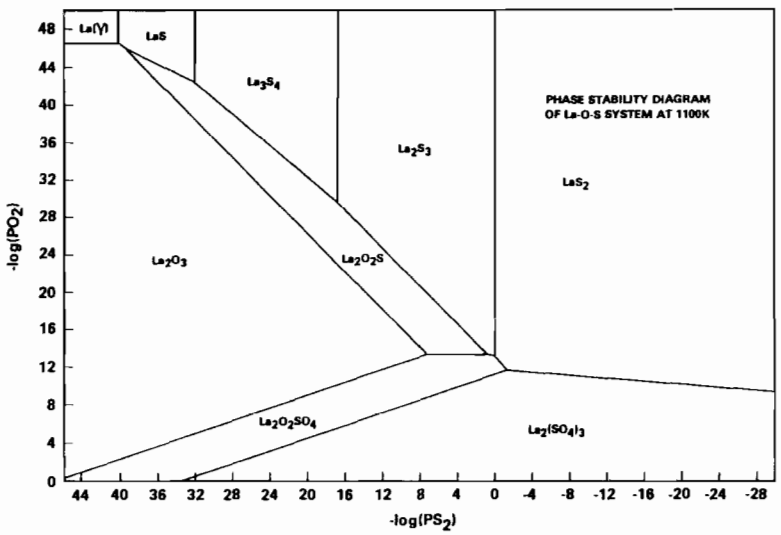


Fig. 1. The La–O–S phase stability diagram at 1100 K [5].

These data were combined with those of Grunzweig [6] for the $La_2(SO_4)_3/La_2O_2SO_4$ equilibrium; Gschneidner *et al.* [3] for $La_2O_3$; Mills [7] for LaS and $La_2S_3$; and Vasileva *et al.* [8] for $LaS_2$. The standard free energy of formation of $La_3S_4$, $\Delta G_f^0$, $La_3S_4$, was taken to be equal to that of $Ce_3S_4$ [10].

For the Ce–O–S diagram, oxygen concentration cells of the type: $Pt(s)/CeO_x(s)$, $Ce_2O_2S(s)$, $Ag(s)$, $Ag_2S(s)/CSZ/Air/Pt(s)$ have been used [9] to generate thermodynamic data on the equilibrium:

$$Ce_2O_2S(s) + (x - 1)O_2(g) = 2CeO_x(s) + 1/2S_2(g) \quad (2)$$

The data were combined with those of Gschneidner and Kippenham [10] for the sulfides; Gschneidner *et al.* [3] for the oxysulfide; Bevan and Kordis [11] for the oxides; and Barin *et al.* [12] for $Ce_2(SO_4)_3$.

In both the La–O–S and Ce–O–S systems there are large uncertainties associated with the standard free energies of formation of some of the compounds and the phase stability diagrams have been constructed using internally consistent data to conform to the phase rule.

*Gaseous Desulfurisation.* The general principles of high temperature gaseous desulfurisation have been outlined elsewhere [1, 13]. In Figs. 1 and 2, for example, the bivariant equilibria $La_2O_3/La_2O_2S$ and $CeO_x/Ce_2O_2S$ represent the limits of desulfurisation which can be attained by contacting gaseous fuels containing $H_2S$ with lanthanum or cerium oxides at 1100 K, the lower the oxygen potential the greater the desulfurisation:

$$2REO_x(s) + 1/2S_2(g) = RE_2O_2S(s) + (x - 1)O_2(g) \quad (3)$$

A gaseous fuel with a room temperature composition of 55% CO, 33% $H_2$, 11% $CO_2$ and 1.1% $H_2S$ by volume can be desulfurised down to about 2 ppm $H_2S$ by $La_2O_3$ and to about 72 ppm $H_2S$ by $CeO_2$, at 1100 K;

| Oxide | TK | log $pO_2$ | log $pS_2$ | ppm $H_2S$ |
|---|---|---|---|---|
| $La_2O_3$ | 1100 | −19.59 | −13.61 | 2.3 |
| $CeO_2$ | 1100 | −19.59 | −10.64 | 72 |

The stability of rare earth sulfates and oxysulfates are of importance during the high temperature regeneration of the oxides by contacting the oxysulfide with air. The decomposition temperatures of the rare earth oxysulfates decrease with increasing atomic number and $La_2O_2SO_4$, with a decomposition temperature of 1943 K, is the most stable of the oxysulfates. Cerium, on the other hand, does not form an oxysulfate and the decomposition temperature of $Ce_2(SO_4)_3$ is 1194 K.

*Graphite Morphology Control in Cast Iron.* The Ce–O–S phase stability diagram at 1500 °C, given in Fig. 3, establishes the liquid iron chemistry, in terms of the Henrian activities of oxygen and sulfur, essential to the control of nodular and compacted graphite in a cast iron melt containing 3.5% C and 2.0% Si treated with cerium [2, 14].

Graphite crystal growth mechanisms are sensitive to soluble impurity concentrations at the parts per million level. Oxygen and sulfur are the principal impurities of technological interest and their activities in treated cast iron melts can be related to the activity of the treatment metal, *e.g.*, Ce, Ca or Mg. At slow cooling rates, such as those obtained in thick sections, where the kinetic undercooling is not significant, graphite morphology can be directly related to Fig. 3.

*Sulfide Morphology Control in Steels.* The phase stability diagram for the Ce–O–S system at 1627 °C [1], given in Fig. 4, establishes the approximate liquid steel chemistry under rare earth deoxidation control and is based on a thermodynamic analysis [4, 15] using the data of Gschneidner and co-workers [3, 10].

The sequence of precipitation of rare earth oxides, oxysulfides and sulfides during the rare earth treatment of a steel of given oxygen and sulfur contents may be determined from this diagram. The bivariant equilibrium $Ce_2O_3/Ce_2O_2S$ determines the conditions

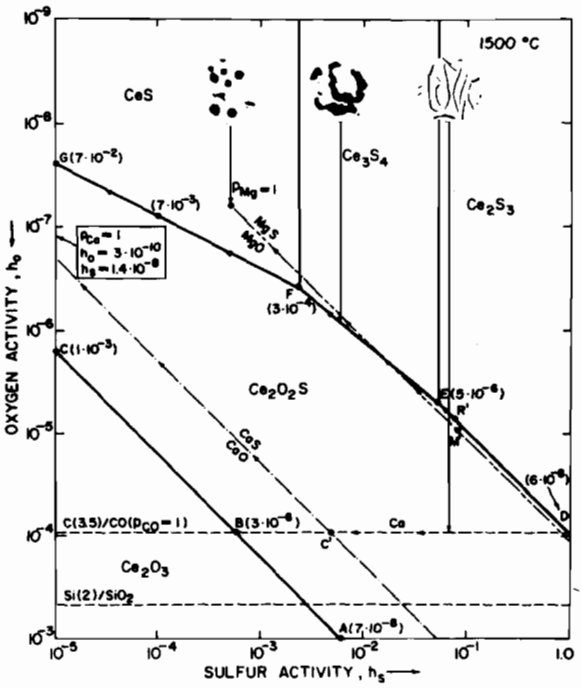


Fig. 3. The Ce–O–S phase stability diagram for graphite morphology control in cast irons at 1500 °C. ($h_i$ is the Henrian activity of a component i referred to the 1 wt.% solution as standard state).

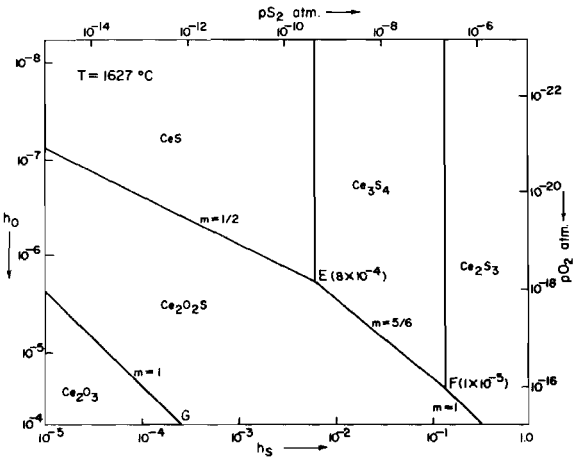


Fig. 4. The Ce–O–S phase stability diagram at 1672 °C for the control of sulfide inclusions in steel.

under which $Ce_2O_3$ may precipitate, *i.e.*, $h_o/h_s > 4.3$. This condition is easily met in the production of modern low sulfur steels.

The authors should like to acknowledge the financial support of the Natural Sciences and Engineering Research Council of Canada, and the Department of Energy, Mines and Resources (CANMET).

1 P. Apte, D. Ghosh and D. A. R. Kay, *Proc. NOH-BOS AIME Conference*, Chicago (1978).
2 S. V. Subramanian, D. A. R. Kay and G. R. Purdy, *AFS Trans.*, 179, (1982) pp. 589–603.
3 K. A. Gschneidner, N. Kippenham and O. D. McMasters, 'Thermochemistry of Rare Earths', IS-RIC, Institute for Atomic Research, Iowa State University, Iowa, 1973.
4 A. Vahed and D. A. R. Kay, *Met. Trans., 7B* (1976) pp. 375–383.
5 R. K. Dwivedi: 'Determination of the Thermodynamics of Rare Earth-Oxygen-Sulfur Systems at High Temperatures'. Ph.D. Thesis, McMaster University (1982).
6 M. Grunsweig, *Ph.D. Dissertation*, Darmstadt, W. Germany. (As reported by H. H. Kelley, *Trans. AIME, 230* (1964) 1623.
7 K. C. Mills, 'Thermodynamic Data for Inorganic Sulfides, Selenides and Tellurides'. Butterworth, London, 1974.
8 I. G. Vasileva *et al., Izv. Akad. Nauk. SSSR, Neorg. Mater., 15(8)*, (1979) 1330.
9 R. K. Dwivedi and D. A. R. Kay, 'Determination of the Standard Free Energy of Formation of $Ce_2O_2S$ and $Y_2O_2S$ at High Temperatures'. *J. Less-Common Metals*. In press.
10 K. A. Gschneidner and N. Kippenham, Report No. IS-RIC-5, Rare Earth Information Centre, Ames, Iowa.
11 D. J. M. Bevan and J. J. Kordis, *J. Inorg. Nucl. Chem., 23*, (1954) 1509.
12 I. Barin, O. Knacke and O. Kubaschewski, 'Thermochemical Properties of Inorganic Substances Supplement'. Springer-Verlag, Berlin, 1976.
13 D. A. R. Kay and W. G. Wilson, 'Methods of Desulfurising Iron and Steel and Gases, such as Stack Gases and the Like'. U.S. Pat. #4,084,960, 1978.
14 S. V. Subramanian, D. S. Ghosh, G. R. Purdy, D. A. R. Kay and J. M. Gray, 'Process for the Production of Vermicular Cast Iron', U.S. Patent #4,227,924, 1980.
15 W. G. Wilson, D. A. R. Kay and A. Vahed, *J. of Metals, 26(5)*, (1974) 14–23.

## E11

## Thermoelectric Properties of $M^{4+}/M^{3+}$ and $MO_2^{2+}/MO_2^{+}$ Redox Couples of Neptunium and Plutonium in Aqueous $HClO_4$ and $HNO_3$ Media

P. BLANC and C. MADIC*

*Institut de Recherche Technologique et de Développement Industriel, Division d'Etudes de Retraitement et des Déchets et de Chimie Appliquée, Department de Génie Radioactif, Service des Etudes de Procédés, Section des Transuraniens, Centre d'Etudes Nucléaires de Fontenay-aux-Roses, B.P. No. 6, 92260 Fontenay-aux-Roses, France*

The thermoelectric properties of redox couples of transuranium elements in acidic, slightly complexing media ($HClO_4$ and $HNO_3$) have been considered. For these elements the redox couples suitable for that study correspond to the reversible $M^{4+}/M^{3+}$ and $MO_2^{2+}/MO_2^{+}$ systems. So only the couples of neptunium and plutonium have been studied with the following precautions. First, the use of an inert atmosphere ($N_2$) prevents the oxidation of $Np^{3+}$ ion. Second, the selection of a pH close to 3.5 minimizes the disproportionation reaction of $PuO_2^{+}$ ion.

Theoretical considerations lead to the conclusion that the electromotive force between two inert electrodes in contact with an aqueous solution containing the reversible redox couple and subjected to two different temperatures is expressed according to:

$$\Delta V = \Delta T \times \epsilon \quad (1)$$

where $\Delta T$ is the gradient of temperature and $\epsilon$ the thermoelectric power of the redox couple which can be written as:

$$\epsilon = \epsilon_o + \frac{R}{nF} \log \frac{[Ox]}{[Red]} + \frac{R}{nF} \log \frac{\gamma_{Ox}}{\gamma_{Red}} \quad (2)$$

Equation (2) is an approximation of the derived of the Nernst equation versus temperature, where the terms possess their usual signification and $\epsilon_o$ is the absolute thermoelectric power proportional to the difference in the standard entropies of the two ions of the redox couples:

$$\epsilon_o = \frac{\Delta S_o}{nF} \quad (3)$$

For all $M^{4+}/M^{3+}$ and $MO_2^{2+}/MO_2^{+}$ redox couples of the neptunium and plutonium elements a check of the validity of equation (1) and of the different terms of equation (2) has been made by studying first, the variation of $\Delta V$ versus the gradient of temperature $\Delta T$ for solutions with constant composition, second,